



A New Toolbox for Generating Realistic Biological Cell Geometries for Electromagnetic Microdosimetry

A. H. Buchali Safiee¹, E. Sharifi², M. Saviz^{3,*}

¹ B.Sc. Student, Biomedical Engineering Department, Amirkabir University of Technology, Tehran, Iran

² M.Sc. Student, Biomedical Engineering Department, Amirkabir University of Technology, Tehran, Iran

³ Assistant Professor, Biomedical Engineering Department, Amirkabir University of Technology, Tehran, Iran

ABSTRACT: Researchers in bioelectromagnetics often require realistic tissue, cellular and sub-cellular geometry models for their simulations. However, biological shapes are often extremely irregular, while conventional geometrical modeling tools in the market cannot meet the demand for fast and efficient construction of irregular geometries. We have designed a free, user-friendly tool in MATLAB that combines several known or new algorithms for easy production of three-dimensional complex cell shapes based on minimum data. We have considered four different methods of creating objects: Generalized Rotation, Super-Formula, 3D reconstruction of 2D parallel cross-sections and branching models. Besides, many transformations such as translation and rotation, Boolean operations for 3D objects including union and intersection, random copy, etc. are also included in the toolbox. By utilizing different methods, our toolbox generates a larger variety of realistic biological geometries, especially tailored for irregular and branching cellular and sub-cellular shapes. We present a group of biological shape examples in this paper. The toolbox can export the geometries to common standard stl or voxel formats to be used for simulations in other software. We have developed an open, user-friendly toolbox, with specialization in cellular and sub-cellular irregular models. This toolbox can provide the essential realistic cellular models for scientific simulations in biomedical engineering, biotechnology, bioelectromagnetics, cell biomechanics, and serve as an educational visualization tool in teaching cell biology. Examples of microdosimetric simulations for electromagnetic exposure to RF frequencies are given and discussed.

Review History:

Received: 2019-05-05

Revised: 2019-12-16

Accepted: 2019-12-17

Available Online: 2020-06-01

Keywords:

MATLAB toolbox

Realistic cell shapes

Three-dimensional

Geometrical modeling

Irregular, open-source

1. INTRODUCTION

Recently, the importance of three-dimensional modeling of cellular shapes has increased in various fields such as Bioelectromagnetics, Biomechanics and developmental Biology. In [1] the necessity to consider a realistic cell shape for computing the induced voltage across cell membranes has been shown, and [2] indicates this for estimating dielectric properties of biological tissues. Also, the importance of cell modeling in developmental biology for evaluation of cell shapes and size is reported in [3]. In pre-2000 studies, computer models of cells were generally limited to simple or multi-layers spherical geometries with homogenous properties.

In 2001, Sebastian and colleagues [4] showed that cell shape and its orientation in electrical field do significantly affect the field penetration into cell compartments. These and other researchers considered multiple-layer spherical, elliptical and cylindrical models in order to examine the intensity of electric fields. The layers were meant as crude

models of internal organelles. Subsequently, in 2002, Walker and his colleagues [5] modeled a layer of epithelial tissue with cells, which contain nucleus, and created a microscopic model of tissue. Beginning in 2003, Weaver and colleagues [6] modeled irregular cells in two dimensions. In this study, each cell contained a membrane, nucleus and cytoplasm. Using the transmission network method provided the possibility of using a nonlinear membrane model in modeling.

In 2006, for the first time, a simple model of the cell with a few simple examples of internal organs such as mitochondria and endoplasmic network was created. This study was designed to investigate the effect of electroporation on cell's components and shows the importance of the presence of organelles, in examination of field in cells [7, 8].

An important work in 2010, that of Huclova and colleagues [8] proved the importance of using realistic cellular shapes instead of simple geometric ones for correct estimation of tissue conductivity. In 2010 Hartinger [9] modeled the skin at microscopic scales in a healthy and patient state with cell and nucleus, and announced the ideal frequency range for the

*Corresponding author's email: msaviz@aut.ac.ir



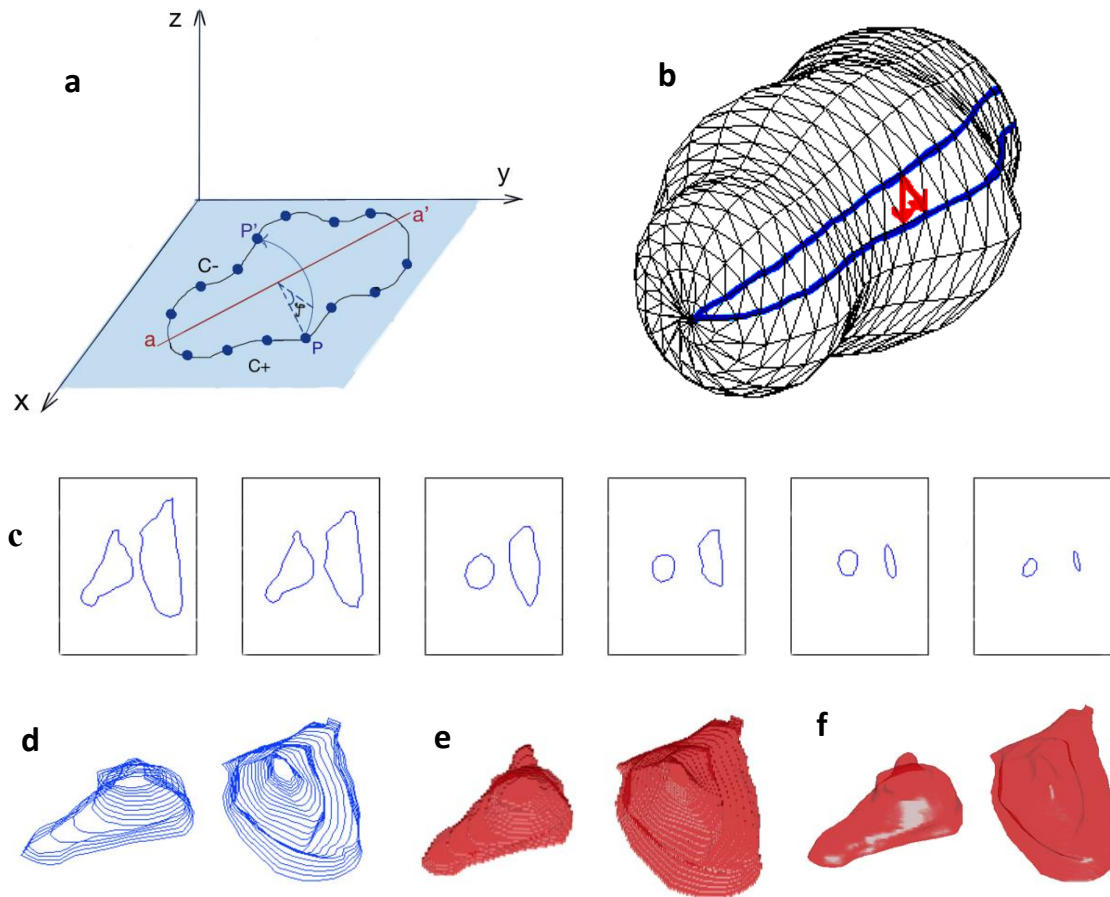


Fig.1. Corresponding to the method of section 2.1: (a) the generalized rotation, consisting of interpolating between the curves on either side of the axis aa' . (b) Surface triangles. One of the middle curves is highlighted in red in red. Small arrows depict the connection scheme to define triangle edges. **Corresponding to the method of section 2.3:** (c) Determination of Shape Boundaries; corresponding cell boundaries for a given cross-section. (d) Polygon Interpolation; ten polygons which are parallel to xy plane has been interpolated between cross-sections (e) Conversion to Binary Values; voxelised matrix of the object has been created. (f) Surface Extraction; the surface of the cell obtained from voxelised object using isosurface techniques

diagnosis of disease is below 10 kHz.

In 2014, the importance of the realistic cellular shapes in modeling led to creation of a toolbox to model realistic geometric shapes based on the cell's microscopic image [10]. Most recently in 2016, it has been shown that realistic cell shape can be crucial, even for results of chemical pathway simulations [11]. Realistic shape modeling has also been indicated in simulating cell migration [12].

In this paper we describe the ability of our toolbox named SAVI in biological modeling, with emphasis on irregular cellular models. Available modeling programs in the market are designed with regard to regular, industrial shapes. Creating smooth but irregular or branching (like neurons or cells with cilia) biological structures with conventional methods becomes very complicated and difficult. This toolbox was devised to tackle the inability of conventional computer modeling tools in construction of realistic geometrical models of irregular biological cell shapes and organelles. The main algorithms for body generation are discussed next. The graphical user interface is also discussed. We then present several examples and compare the tool efficiency with a well-known industrial shape modeler. The tool can provide the

essential realistic cellular models for scientific simulation or visualization in biomedical engineering, cell biomechanics or bioelectromagnetics, and serve as an educational visualization tool for teachers of biology and bioengineering.

2. METHODS

In this toolbox we utilize four different methods for creating models, in order to include the vast number of biological shapes. The user could use each of these methods or their combination to create a model. Also, there are many other tools that may help the user to alter, transform, and combine the obtained models. We describe these methods below. Considering restrictions in journal pages, we avoid details on other well-known methods such as translation, rotation, etc.

2-1- Generalized Rotation

This method is based on a single 2D image [10]. The user determines the boundary of the object -either manually or automatically- by selecting a number of points. Automatic selection of points is possible by utilization of an approach in image processing field called Snake algorithm [13]. In Fig. 1(a), which is a 2D image on $x-y$ plane, the boundary

of object. is determined by a set of points. Then, the user defines a rotation axis (aa') that separates the boundary to two parts (C_- and C_+). In this method the algorithm finds corresponding points between C_- and C_+ , and rotates the points on C_+ ($\varphi = 0$) around the aa' axis so as they match to their correspondences on C_- ($\varphi = 180$). For example, point P on curve C_+ , rotates around aa' to connect point P' on curve C_- . These rotations create a number of intermediate curves. Their number depends on the angular step. In the final step, the algorithm connects these points to create the surface of the 3D object. Assume we define the set of points as Eq. (1), then for creating the surface triangles we apply Eq. (2) and Eq. (3) for all the points, so that the triangles will be formed.

$$P_{n,i} = (x_{n,i}^{3D}, y_{n,i}^{3D}, z_{n,i}^{3D}) \tag{1}$$

$$P_{n,i} \rightarrow P_{n,i+1} \tag{2}$$

$$P_{n,i} \rightarrow P_{n+1,i+1} \tag{3}$$

2-2- Super Formula

This method is provided in [14], and is based on the determination of some parameters, which gives this method a little flexibility. The user defines the parameters of Super Formula and the algorithm puts these parameters in Eq. (4-9), to create the surface points. In the final step, the surface triangles are created exactly in the same way of Generalized Rotation method.

$$P_1 = \left| \frac{1}{a} \cos \left(m \frac{\varphi}{4} \right) \right|^{n_2} + \left| \frac{1}{b} \sin \left(m \frac{\varphi}{4} \right) \right|^{n_3} \tag{4}$$

$$P_2 = \left| \frac{1}{a} \cos \left(m \frac{\theta}{4} \right) \right|^{n_2} + \left| \frac{1}{b} \sin \left(m \frac{\theta}{4} \right) \right|^{n_3} \tag{5}$$

$$r_1 = \frac{1}{\sqrt[n_1]{|P_1|}}, r_2 = \frac{1}{\sqrt[n_1]{|P_2|}} \tag{6}$$

$$x = r_1 \cos \varphi . r_2 \cos \theta \tag{7}$$

$$y = r_1 \sin \varphi . r_2 \cos \theta \tag{8}$$

$$z = r_2 \sin \theta \tag{9}$$

Where the quantities θ, φ are the elevation and azimuth angles in spherical coordinates and n_1, n_2, n_3 and m are integer parameters controlling shape geometry.

2-3- Three-Dimensional reconstruction of parallel cross-sections

When a number of parallel cross-sections of an object are available, SAVI can reconstruct the 3D object by using this process. In the first step, the user should load all the cross-sections and determine the object boundary in each

image, by using manual or automatic selection of boundary. The next step is to estimate a number of curves between these cross-sections in order to have a smooth output after reconstruction. For this purpose, the algorithm puts a specific number of points on each cross-section's boundary and finds corresponding points between cross-sections, by using a minimum distance algorithm. Then by utilizing Spline we estimate some points between corresponding points, and by connecting them together the middle curves are formed. The algorithm generates the surface of the object through 3D binary matrix of the object (3D voxelised matrix), which itself is created through changing the curves data into 2D binary matrices; matrices with binary values (0 for Outside and 1 for Inside the curve). Fig. 1(c-f) shows the process of applying this method on contours of six parallel cross-sections of a cell step by step.

2-4- Branching Models

The last method for creating models is allocated to biological branching structures. The user can create the body part for the branching structure by using one of the previous methods. Fig.2 (a) shows the main steps for formation of a branching model. The first step is to create the 3D branching model using L-systems[15]. In brief, L-systems create complex objects by successively replacing parts of a simple initial object using a set of rewriting rules or productions. We have set some predetermined rules that can be used for biological modeling. Although the output models of the L-systems are 3D, they don't have volumes. The algorithm creates a volume for each branch. The volume of each branch relates to the branch order of that branch; higher order branches should have a larger diameter. Hence the second step is the determination of the branch orders of the L-system model.

We assign orders to branches iteratively according to the adjacent branch orders (branch orders for branches that are joined to each other in a particular node). For ordering the branches in L-system model, we first find the nodes that their node orders are equal to one (float nodes). These float nodes are attached to the branches that their branch orders are equal to one. Then we use an iterative function for all nodes to find branch orders higher than one. To understand how this functions work, assume that N numbers of branches are connected together in a particular node. We know the branch orders for (N-1) branches and we want to determine the branch order for the unknown one. If the maximum of all (N-1) branch orders is exclusive, the branch order of the last branch is equal to the Max; otherwise its branch order is equal to (Max+1).

After determination of branch orders, we need to create a volume for L-system model. For this purpose, we used voxels (volume cell. The numbers of voxels, which determine the branch diameter, are related to branch orders. In the final step, we obtain the surface of the object from the voxelised object, using MATLAB functions, Isosurface and Isocaps.

2-5-Transform Tools

We have considered a group of tools that may help to

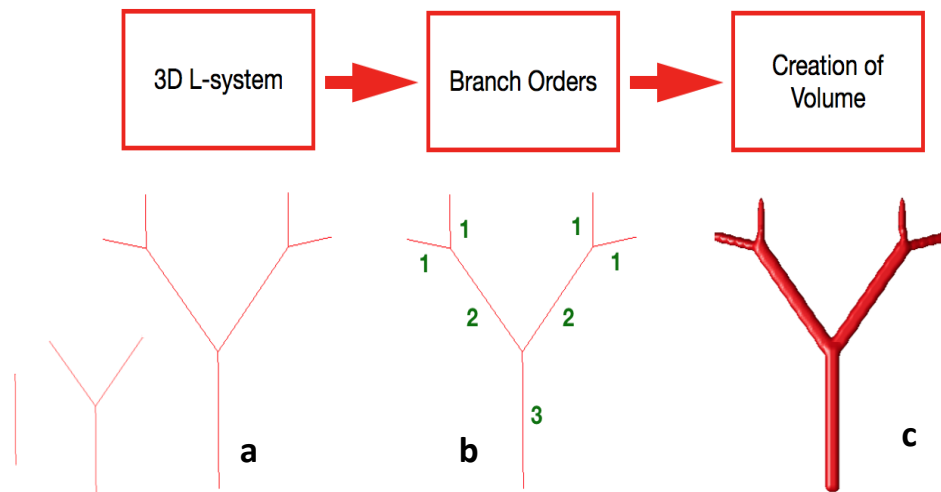


Fig.2. (a) L-system model: The L-system process for creating a simple example of branching object is shown. (b) Branch Ordering: branch orders are obtained for the example. (c) Creation of volume: Volume has been added to branches according to their branch orders by using 3D voxelised matrix.

make the necessary changes to created shapes. In this part we review some of the most important transform tools:

2-5-1 Boolean Operations

This transformer can obtain Union or Intersection of two or more objects. The Subtraction of two objects is also possible with this transformer. We first create a three-dimensional binary matrix (voxelised matrix) for each object, which represents them. Then we apply these Equations that are for combination of two 3D matrices (A and B):

$$\text{Union} : (A + B) \geq 1 \quad (10)$$

$$\text{Intersection} : (A \cdot B) > 0 \quad (11)$$

$$\text{Subtraction} : (A - B) \geq 0 \quad (12)$$

2-5-2 Random Copy

In many Biological structures, we need to randomly copy a high number of objects inside another one. For instance, many organelles are randomly distributed in high quantities in a cell. By using this transformation, the user chooses the area of copy and the number of copies, and the algorithm will randomly copy the objects.

Many other conventional tools that are available in other modeling software such as Scale, Translate, Rotate, Copy, Convex Hull, Add Random Points, view Cross-sections, etc. are also available in SAVI.

2-6- Input/output

For the purpose of connecting SAVI to other software, it can create outputs and accept inputs in STL and VOXEL formats as well as the main MATLAB format. STL format is created by [16]. In VOXEL format, we create a 3D binary matrix for each object using [17]. Also, we create a combined matrix, which represents all objects in only one 3D matrix;

each object has a specific value in that matrix. The User can select the Cellular Volume Fraction (CVF) for the combined matrix, which determines the empty space to be included outside the cell, as well.

3. SOFTWARE

To create a user-friendly toolbox, we have used the graphical user interface (GUI) builder of MATLAB. Our toolbox consists of many GUIs that are connected to the main GUI, and they will appear when the user presses their related button. For example if we select an object and press the multiple copy button, its corresponding GUI will appear. Fig. 3 shows the main GUI for SAVI, which includes six different panels, shortly described below:

Create: This panel is allocated to five methods of generating new object; Generalized rotation, Super formula, 3D reconstruction of 2D parallel cross-sections, Branching models and basic objects.

View: This panel dedicated to examining all the objects, individual objects or cross-sections of the objects.

Objects: This panel shows all the created objects in a list. The selected object of this list will be highlighted with a blue color, while all the other objects are shown in red. Also, the user can delete, restore or rename the selected object using the modules of this panel.

Graphic: This panel shows all the generated models in a 3D figure.

Reports: This panel informs the user of the outcomes.

Along with these panels, there are tabs such as *create a new project*, *save a project* and *Load a project*, and menus such as *export*, *import* and *help* that are included in the main GUI.

4. RESULTS

In this part, we constructed two groups of examples that show ability of SAVI in biological modeling.

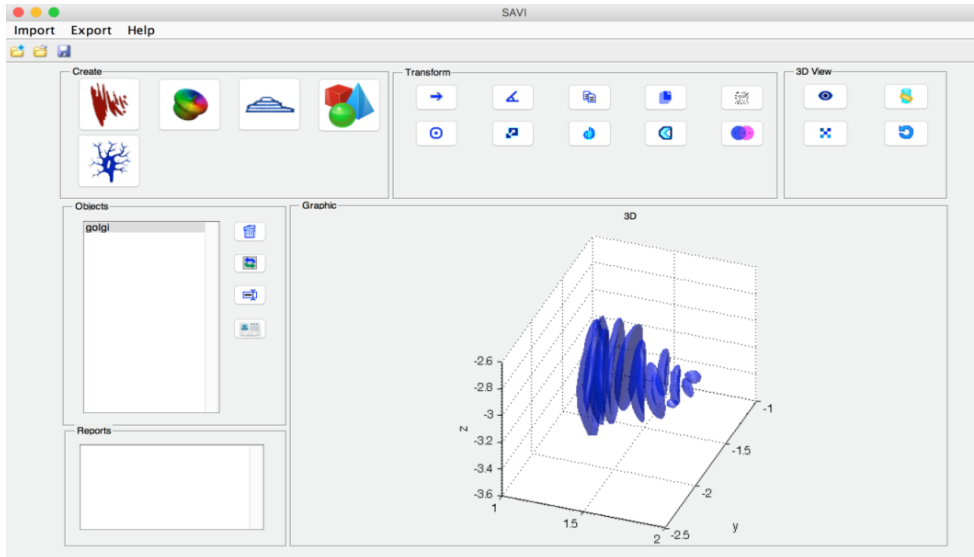


Fig. 3. The main graphical user interference of the SAVI toolbox.

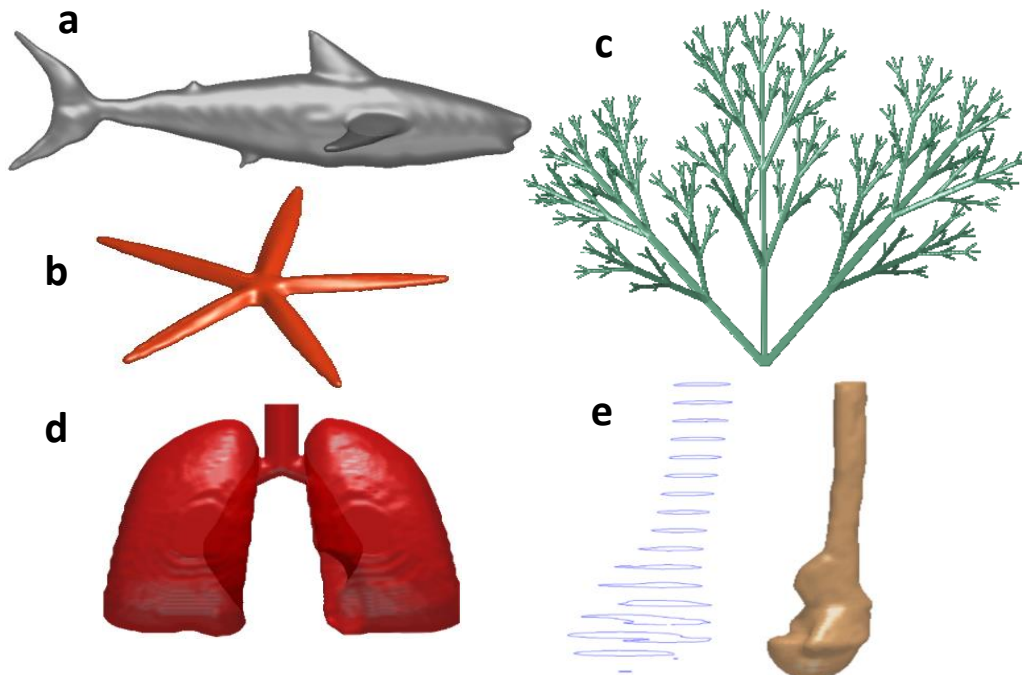


Fig.4. (a) Shark: This model is obtained by Union of several parts which are created by Generalized Rotation method. (b) Starfish: This model is obtained by Super Formula method. (c) Coral: This model is obtained by using L-Models method. (d) Lungs: This model is obtained by Union of several parts which are created by Generalized Rotation method. (e) Femur bone: This model is obtained by using 3D reconstruction of 2D parallel cross-sections. The parallel contours of cross-sections are also shown.

4-1-Biological Organs

The first category is not limited to a specific group of biological organs. Fig. 4 shows biological models that we obtained by using different creating methods.

4-2-Cell and Organelles

The main purpose of this toolbox is cell modeling. Since cellular shapes are irregular, SAVI provides various methods to meet the demand for flexibility and versatility in constructing

irregular geometries. Fig. 5 shows a vast number of cellular and subcellular models.

5. DISCUSSION

Conventional modeling toolboxes are created based on an industrial mentality. This purpose causes the concentration on regular geometries, which are common in industrial models. On the other hand, biological shapes are mostly irregular. Hence the use of conventional methods for biological purposes

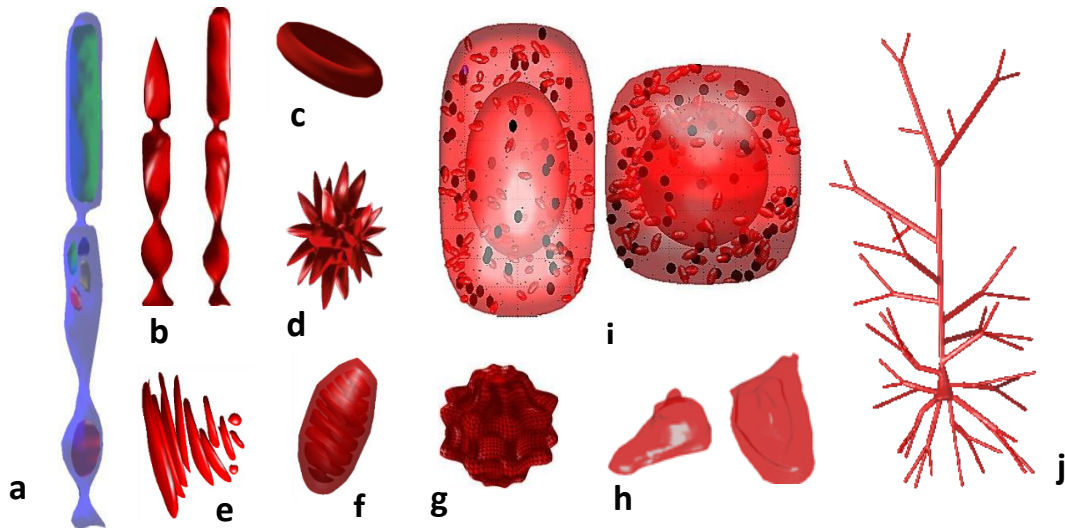


Fig.5 (a) A rod cell with filled outer segment and several mitochondria, and a nucleus, (b) Cone and rod cells, (c) Normal red blood cell, (d) Small white blood, (e) Golgi body organelle, (f) Mitochondrion organelle, (g) Cell with protrusions, (h) Chinese hamster ovary cell, (i) Two view of geometric model of the basal cortex cubic cell in the skin epidermis with internal organs, (j) Pyramidal neuron.

Table 1. Estimated time that user spends on Shark and Coral modeling in SAVI toolbox in MATLAB R2013a for mac.

Shark		Coral	
Steps	Estimated time (min)	Steps	Estimated time(min)
Generalized rotation	4	L-system design	10
Scale	2	Body creation	1
Rotation	1	Position of branches	1
Translation	1	Orientation of branches	1
Union	1	Run time	2
Total time	9 minutes	Total time	15 minutes

is unacceptable. SAVI toolbox is devised based on irregular shapes mentality; therefore the user can obtain the realistic and flexible models of irregular objects, which are impossible or difficult to generate with conventional modeling toolboxes. We have shown the ability of SAVI in creating irregular biological shapes in Fig.4, and also the strength of this toolbox in cellular modeling is indicated in Fig.5.

Another advantage of SAVI compared with other modeling toolboxes is the ease in working and modeling, which results

in minimum time for generating complex biological objects. Table1 shows the estimated time that a user spends to create two complex objects, shark and coral, which are shown in Fig.4.

One of the factors that helps saving time is the ability to keep objects coordinate according to the 2D micrographs. For example, in modeling a cell within its organelles from a 2D micrograph, the user models each organelle separately but in the final model, the coordinates are the same as the 2D model,

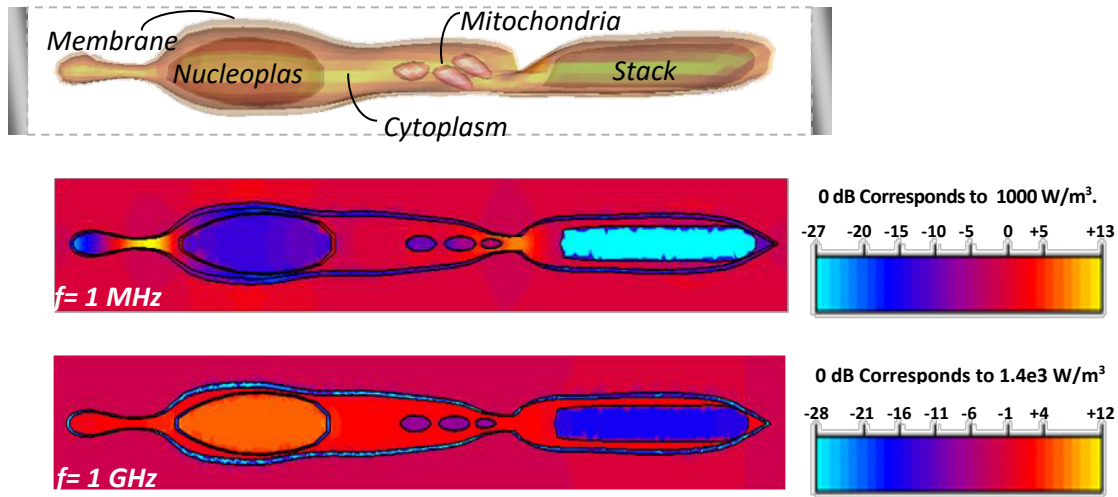


Fig.6. Example simulation: The model retinal rod cell and volume power loss density within the cell exposed to electric fields at frequencies of 1MHz and 1GHz.

so there is no need to spend time to correct the coordinates.

Although we have attempted to create a complete toolbox for cellular and biological modeling, SAVI similar to other toolboxes needs to be upgraded continually. At the moment, there are certain biological and cellular shapes that SAVI toolbox cannot model, and we hope to consider them in the next versions of the toolbox. For instance, SAVI currently cannot model spiral shapes like snails or seahorses and serpentine shapes like snakes with the same ease as with other models. As a result, some other methods for creating objects should be included in SAVI's next versions. Also, to embrace a larger group of branching structures such as Purkinje cells, more L-systems rules can be included. Finally, more export and import formats can be incorporated in future versions of SAVI.

It is instructive to compare the modeling capabilities with [14]. The superformula in [14]. In addition to avoiding the regularities and symmetries in [14], the combination of methods in this toolbox allows for much more flexible shape design and visualization. Most importantly, the toolbox can implement branched structures and shelled compartments, much an improvement over [12] and [14]. An open-source code of the toolbox is available at [18].

6. MICRODOSIMETRY

Obtaining accurate results for electromagnetic field distributions at cellular scales (Microdosimetry) has been of interest recently [4]. This requires accurate modeling of cell shapes and can now be more easily provided by our toolbox. An example is now given regarding the microwave exposure of retinal rod cells (light-sensing cells on the retina).

The cell model is shown in Fig. 2. The cell diameter is almost $1.7 \mu m$ and its length is about $30 \mu m$. The model is stimulated by a capacitive arrangement, consisting of two parallel plates $36 \mu m$ apart. The electrodes are filled in between with material properties of physiological saline. The model

is solved in the electromagnetic simulation software CST EMS* with tangential boundary conditions on four lateral sides, which implicitly assumes periodicity in all directions. Incident field lies along the cell axis and has an intensity of 77 V/m . This is an estimation of the electric field induced in the head by a GSM mobile phone with a maximum allowable SAR of 1.6 W/Kg . Dielectric permittivity and conductivity properties used for the models are obtained from references [19-21] which are for $f = 1 \text{ MHz}$, and $f = 1 \text{ GHz}$ respectively;

$$\epsilon_{\text{cytoplasm}} = 184,64 \quad \sigma_{\text{cytoplasm}} = 0.4, 1.17 \text{ S/m},$$

$$\epsilon_{\text{Membrane}} = 12.8, \sigma_{\text{Membrane}} = 5.6 \times 10^{-5} \text{ S/m},$$

$$\epsilon_{\text{Ex.Cellular}} = 48,47.9 \quad \sigma_{\text{Ex.Cellular}} = 0.3, 0.4 \text{ S/m},$$

$$\epsilon_{\text{Nucleoplasm}} = 90, 61.6,$$

$$\sigma_{\text{Nucleoplasm}} = 2.8, 3.6 \text{ S/m}, \epsilon_{\text{Nuc.Envelope}} = 160,$$

$$\sigma_{\text{Nuc.Envelope}} = 0.011 \text{ S/m}, \epsilon_{\text{Stack}} = 18,$$

$$\sigma_{\text{Stack}} = 10^{-6} \text{ S/m}, \epsilon_{\text{Mito}} = 54, \sigma_{\text{Mito}} = 0.12 \text{ S/m}.$$

The distributions of volume electric loss density are given in Fig. 6. An important observation is that electric field is increased within the synaptic "neck" of the cell, twenty times more intense than the average loss in the tissue (the extracellular medium and most of the cytoplasm). This is because free-charges have to travel through a smaller channel at the neck, surrounded by almost-insulating (capacitive) cell membranes, which results in higher current density and thus higher electric field intensity. This type of amplification is absent at higher frequencies, where displacement current become dominant relative to free-charge (ionic) currents, and the impedance of membrane capacitors decreases.

Consequently, currents are no more bounded by membranes and the neck-amplification disappears, as can be observed in Fig. 6, in the results at $f = 1$ GHz.

Another interesting aspect is the shielding of the interior of organelles at lower frequencies by non-conducting membranes. Since the membranes are only weakly conducting, they block currents from penetrating into these compartments. This shielding is also a low-frequency phenomenon, and is absent at higher frequencies (Fig.6).

7. CONCLUSION

We have reported a new modeling toolbox which has special abilities to model irregular biological shapes. We have also described different geometric design methods that we believe can include a vast number of biological organs, especially cellular and sub-cellular shapes. SAVI is a user-friendly graphical user interface, which incorporates all the tools introduced. These tools find application in bioelectromagnetics, biomechanics and developmental biology and also as visualization tools for teaching biology and bioengineering. They produce various smooth, irregular shapes that are not as easily generated by the conventional industrially optimized CAD tools. The outputs are in standard formats and can be used in other modeling software.

8. ACKNOWLEDGEMENT

We would like to thank Peyman Gholami for his code-contribution in this work.

9. CONFLICT OF INTEREST

The authors declare that there is no conflict of interests regarding the publication of article.

REFERENCES

- [1] G. Pucihar, T. Kotnik, B. Valič, D. Miklavčič, Numerical determination of transmembrane voltage induced on irregularly shaped cells, *Annals of biomedical engineering*, 34(4) (2006) 642.
- [2] S. Huclova, D. Erni, J. Fröhlich, Modelling and validation of dielectric properties of human skin in the MHz region focusing on skin layer morphology and material composition, *Journal of Physics D: Applied Physics*, 45(2) (2011) 025301.
- [3] A. Chakraborty, R.K. Yadav, G.V. Reddy, A.K. Roy-Chowdhury, Cell resolution 3d reconstruction of developing multilayer tissues from sparsely sampled volumetric microscopy images, in: 2011 IEEE International Conference on Bioinformatics and Biomedicine, IEEE, 2011, pp. 378-383.
- [4] J. Sebastián, S. Munoz, M. Sancho, J. Miranda, Analysis of the influence of the cell geometry, orientation and cell proximity effects on the electric field distribution from direct RF exposure, *Physics in Medicine & Biology*, 46(1) (2001) 213.
- [5] D. Walker, B. Brown, R. Smallwood, D. Hose, D. Jones, Modelled current distribution in cervical squamous tissue, *Physiological Measurement*, 23(1) (2002) 159.
- [6] T.R. Gowrishankar, J.C. Weaver, An approach to electrical modeling of single and multiple cells, *Proceedings of the National Academy of Sciences*, 100(6) (2003) 3203-3208.
- [7] T.R. Gowrishankar, A.T. Esser, Z. Vasilkoski, K.C. Smith, J.C. Weaver, Microdosimetry for conventional and supra-electroporation in cells with organelles, *Biochemical and biophysical research communications*, 341(4) (2006) 1266-1276
- [8] S. Huclova, D. Erni, J. Fröhlich, Modelling effective dielectric properties of materials containing diverse types of biological cells, *Journal of Physics D: Applied Physics*, 43(36) (2010) 365405.
- [9] A.E. Hartinger, R. Guardo, V. Kokta, H. Gagnon, A 3-D hybrid finite element model to characterize the electrical behavior of cutaneous tissues, *IEEE Transactions on Biomedical Engineering*, 57(4) (2009) 780-789.
- [10] M. Saviz, R. Faraji-Dana, Realistic cell and organelle shape modeling for computational bioengineering: A new open-source toolbox, in: 2014 22nd Iranian Conference on Electrical Engineering (ICEE), IEEE, 2014, pp. 1859-1862.
- [11] F. Sayyid, S. Kalvala, On the importance of modelling the internal spatial dynamics of biological cells, *Biosystems*, 145 (2016) 53-66.
- [12] W.R. Holmes, L. Edelstein-Keshet, A comparison of computational models for eukaryotic cell shape and motility, *PLoS computational biology*, 8(12) (2012) e1002793.
- [13] M. Kass, A. Witkin, D. Terzopoulos, Snakes: Active contour models, *International journal of computer vision*, 1(4) (1988) 321-331.
- [14] J. Gielis, A generic geometric transformation that unifies a wide range of natural and abstract shapes, *American journal of botany*, 90(3) (2003) 333-338.
- [15] P. Prusinkiewicz, A. Lindenmayer, *The algorithmic beauty of plants*, (Springer-Verlag: New York), (1990).
- [16] Sven, stlwrite - Write binary or ascii STL file., in *Matlab Central*, 2012.
- [17] A.H. Aitkenhead, Polygon mesh voxelisation, in *Matlab Central*, 2010.
- [18] M. Saviz, SAVI toolbox ver 2.00, in *www.bioelectromag.ir*, 2017.
- [19] J. Gimsa, T. Müller, T. Schnelle, G. Fuhr, Dielectric spectroscopy of single human erythrocytes at physiological ionic strength: dispersion of the cytoplasm, *Biophysical journal*, 71(1) (1996) 495-506.
- [20] R.P. Joshi, Q. Hu, K.H. Schoenbach, Modeling studies of cell response to ultrashort, high-intensity electric fields-implications for intracellular manipulation, *IEEE Transactions on Plasma Science*, 32(4) (2004) 1677-1686.
- [21] Molaei, M. Saviz, R. Faraji-Dana, Detailed modeling and numerical analysis of photoreceptor cells exposed to electromagnetic fields, in: 2011 19th Iranian Conference on Electrical Engineering, IEEE, 2011, pp. 1-6.

HOW TO CITE THIS ARTICLE

A. H. Buchali Safiee, E. Sharifi, M. Saviz, A New Toolbox for Generating Realistic Biological Cell Geometries for Electromagnetic Microdosimetry, *AUT J. Elec. Eng.*, 52(1) (2020) 89-96.

DOI: [10.22060/ej.2019.16213.5282](https://doi.org/10.22060/ej.2019.16213.5282)

